

Description of Wind/Waves/RAD1 L3
Direction-Finding (DF) data production

X. Bonnin S. Hoang B. Cecconi

12/04/2022 (draft)

Contents

1	General	4
1.1	Scope of this document	4
2	Wind/Waves instrument overview	5
2.1	About Waves experiment	5
2.2	About Waves RAD1 receiver	5
3	Direction-finding (DF) inversion method	7
3.1	Assumptions	7
3.2	Source parameters derived from SUM mode data (synthesized dipole)	8
3.2.1	Basic formulas	8
3.2.2	Source intensity	10
3.2.3	Source azimuth angle	10
3.2.4	Source colatitude angle	11
3.2.5	Modulation rate	11
3.2.6	Source angular radius	12
3.3	Source parameters derived from SEP mode data (equatorial dipole)	13
3.3.1	Basic formulas	13
3.3.2	Source intensity	15
3.3.3	Source azimuth angle	15
3.3.4	Source colatitude angle	15
3.3.5	Modulation rate	15
3.3.6	Source angular radius	16
4	Antenna calibration	17
4.1	Basic formulas	17
4.2	Antenna calibration steps	18
	Appendices	20
A	DF computational data	20
A.1	Input data overview	20
A.2	Output data overview	20
B	Reference frames	22
B.1	Wind spacecraft reference frame	22

B.2	Reference frame used for DF output angles	23
C	Determination of effective antenna length for synthesized dipole . . .	24
C.1	Analysis of signal amplitude over time	24
C.2	Effective antenna length for synthesized dipole	26
C.3	Waves antenna facts	26

1 General

1.1 Scope of this document

This document presents the direction-finding (DF) inversion method applied at LESIA (Observatoire de Paris - PSL), in order to compute the L3 DF parameters from the RAD1 receiver data of the Wind/Waves experiment (Bougeret et al. 1995).

The inversion method is based on the work by Sang Hoang, which is adapted from the study of Manning & Fainberg (1980). The resulting DF parameters are only valid for unpolarized extended radio sources with uniform brightness. The technique is particularly appropriate for the analysis of type III solar radio bursts observed at frequencies below $1MHz$.

The intensity calibration in absolute physical units (i.e., $W/m^2/Hz$) is described in the section 4.

2 Wind/Waves instrument overview

This section gives an overview of the Wind/Waves instrument. More details about the Wind/Waves experiment can be found in Bougeret et al. (1995) and Sitruk & Manning (2003).

2.1 About Waves experiment

The Wind spacecraft was launched on November 1, 1994 to perform Solar Wind and Earth environment observations. The 3 seconds spinning spacecraft has three electrical dipoles X, Y and Z, used as sensors by the Waves experiment to measure radio signals between few Hz and tenth of MHz:

- Z dipole (hereafter also named axial antennas) is aligned with the spin axis of the spacecraft. The tip-to-tip physical length of the Z dipole is 2×4.3 meters before Nov. 6 1996 and 2×4.65 meters after.
- X rotating dipole (hereafter also named equatorial antennas) is in the spacecraft equatorial plane. The tip-to-tip physical length of the X dipole is 2×50 meters after the deployment on Nov. 1994. Nevertheless, the dipole had known two brutal falls of the signal level measured, respectively on Aug. 4 2000 and Sept. 25 2002. These events are supposed to be caused by the impact of micrometeoroids on the X antennas, breaking partially the latter. An estimation of the new X antenna effective length after each break is given in the appendix C.2.
- Y rotating dipole is in the spacecraft equatorial plane and has a tip-to-tip physical length of 2×7.5 meters.

Figure 2 gives a schematic representation of the Waves antennas in the Wind spacecraft reference frame.

2.2 About Waves RAD1 receiver

The RAD1 receiver of the Wind/Waves experiment can acquire data over 256 frequencies between 20 and 1040 kHz with a 4-kHz bandwidth. The receiver measures

the signals coming from three electrical dipoles X, Y and Z via three different channels **s**, **sp** and **z**. More specifically:

- When the RAD1 receiver is configured to work in the SUM mode, the channel **s** provides the sum of the signals from the X and Z dipoles. In the SEP mode, the **s** channel is connected to the X dipole only.
- The channel **sp** provides the same signal than in the **s** channel, but with a phase shift of ~ 90 deg.
- The channel **z** is connected to the Z dipole.

The receiver can be configured into three different modes:

- LIST mode. This mode is mainly aimed to analyze radio source characteristics using the modulation of the signal. For a given frequency and during a period of time close to a spacecraft rotation (~ 3 seconds), the signal is acquired with a high enough sampling rate to observe the modulation effect on the radio emission. Acquisition is performed for a given list of frequencies defined by command. The higher frequencies are recored with higher time resolutions.
- SWEEP mode, where the signals are linearly acquired over up to 256 frequencies using a incremental frequency step Δ_f
- FREEZE mode. Special mode to measure at a given frequency.

In the present case the inversion method is only applied when the RAD1 receiver is tuned to the LIST mode¹.

¹The LIST and SUM modes are used most of the time on-board.

3 Direction-finding (DF) inversion method

The section presents the direction-finding inversion method used to generate Waves RAD1 L3 DF data. The terms and definitions in Manning & Fainberg (1980) are also applied in the present document.

The appendix A.1 lists the actual values of the input parameters used in the algorithm. Except if it is explicitly mentioned all angles are given in radians.

3.1 Assumptions

The method is only applicable under the following conditions:

- Short dipole assumption is valid¹.
- Z axial antennas are not tilted²
- Radio source is unpolarized³.
- Direction-finding parameters are computed assuming a uniform brightness conical radio source
- Radio source signal at a given frequency remains constant over a spacecraft rotation⁴
- Galaxy radio emission is considered as isotropic⁵. This assumption is required to apply the calibration method described in the chapter 4.

¹The short dipole assumption is valid for $2l \ll \lambda/2$, where $2l$ is the total dipole length and λ the source wavelength. This condition is fulfilled in RAD1 frequency range.

²It corresponds to $\sigma_a = \sigma_b = 0$ using relations in Fainberg et al. (1985).

³i.e., Stokes parameters $V = Q = U = 0$

⁴This assumption is valid for solar type III radio burst. However, Waters et al. (2021) has showed it is not applicable for Auroral Kilometric Radiation (AKR) observed at Earth.

⁵It has been shown that the galaxy radio emission is not fully isotropic, but the assumption is good enough for the current situation and the total response of a low-gain antenna can be estimated with reasonable accuracy, i.e. to a factor of 2 or better (see for instance Dulk et al. (2001) for more details).

3.2 Source parameters derived from SUM mode data (synthesized dipole)

3.2.1 Basic formulas

According to equation 23 in Manning & Fainberg (1980), the voltage power spectral density $P_{syn}(t)$ measured at time t and at a frequency f by the receiver in the SUM mode - connected to the synthesized dipole - can be expressed as:

$$P_{syn}(t) = P[P_0 + P_1 \cos(\omega t - \phi) + P'_1 \sin(\omega t - \phi) + P_2 \cos 2(\omega t - \phi) + P'_2 \sin 2(\omega t - \phi)] \quad (3.1)$$

Where $\omega = 2\pi/T_{spin}$ with T_{spin} is the spacecraft spin period in seconds. ϕ is the azimuth angle of the source center in radians. $P = G_0 Z_0 S$ with G_0 is the system gain, Z_0 is the permittivity of the vacuum and S is the flux density of the radio source in $W/m^2/Hz$ measured at the spacecraft location⁶.

P_0, P_1, P'_1, P_2 and P'_2 terms for a synthesized dipole are defined by (Manning & Fainberg 1980):

$$P_0 = \frac{1}{3}(R^2 + 1) - \frac{D}{24}(R^2 - 2)(1 - 3 \cos^2 \theta) - \frac{Q}{24}(R^2 - 2)[2 - D(1 - 3 \cos^2 \theta) - 6 \cos \gamma \cos 2\theta] \quad (3.2)$$

$$P_1 = -\frac{1}{4}R \sin 2\theta \cos \delta [D + Q(4 \cos \gamma - D)] \quad (3.3)$$

$$P'_1 = -\frac{1}{2}R(1 + \cos \gamma) \sin \theta (U \cos \delta - V \sin \delta) \quad (3.4)$$

$$P_2 = -\frac{1}{8}R^2 [D \sin^2 \theta - Q(2 + 2 \cos \gamma \cos 2\theta + D \sin^2 \theta)] \quad (3.5)$$

$$P'_2 = \frac{1}{4}R^2 U \cos \theta (1 + \cos \gamma) \quad (3.6)$$

Where R is the gain ratio. $D = \cos \gamma + \cos^2 \gamma$, with γ is the angular radius of the source in radians ($|\gamma| \leq \pi/2$). θ is the colatitude angle of the source (i.e., zenith angle). δ the phase shift in radians. (V, Q, U) are the Stokes parameters for a partially polarized incoming wave.

⁶ S corresponds physically to the I Stokes parameter (see for instance in Kraus (1966)).

3.2. SOURCE PARAMETERS DERIVED FROM SUM MODE DATA (SYNTHESIZED DIPOLE)9

For the axial antennas, the voltage power spectral density $P_Z(t)$ measured at time t and at frequency f by the receiver on the \mathbf{z} channel is:

$$P_Z(t) = G_0 Z_0 S(P_0)_{R=0} = PP_Z \quad (3.7)$$

Where $S(P_0)_{R=0}$ is the source intensity measured by the Z antennas aligned with the spin axis. According to Manning & Fainberg (1980), the term P_Z can be expressed as:

$$P_Z = \frac{1}{3} + \frac{D}{12}(1 - 3 \cos^2 \theta) + \frac{Q}{12}[2 - D(1 - 3 \cos^2 \theta) - 6 \cos \gamma \cos 2\theta] \quad (3.8)$$

Assuming an unpolarized source (i.e. $Q = V = U = 0$), the terms $P_0, P_1, P'_1, P_2, P'_2$ and P_Z become:

$$P_0 = \frac{1}{3}(R^2 + 1) - \frac{D}{24}(R^2 - 2)(1 - 3 \cos^2 \theta) \quad (3.9)$$

$$P_1 = -\frac{1}{4}RD \sin 2\theta \cos \delta \quad (3.10)$$

$$P'_1 = 0 \quad (3.11)$$

$$P_2 = -\frac{1}{8}R^2 D \sin^2 \theta \quad (3.12)$$

$$P'_2 = 0 \quad (3.13)$$

$$P_Z = \frac{1}{3} + \frac{D}{12}(1 - 3 \cos^2 \theta) \quad (3.14)$$

Relations 3.9 to 3.13 lead to simplify the expressions 26 in Manning & Fainberg (1980) as:

$$F_0 = PP_0 \quad (3.15)$$

$$F_1 = \frac{1}{2}PP_1 \cos \phi \quad (3.16)$$

$$F'_1 = \frac{1}{2}PP_1 \sin \phi \quad (3.17)$$

$$F_2 = \frac{1}{2}PP_2 \cos 2\phi \quad (3.18)$$

$$F'_2 = \frac{1}{2}PP_2 \sin 2\phi \quad (3.19)$$

$$F_Z = PP_Z \quad (3.20)$$

The terms F_0 , F_1 , F'_1 , F_2 and F'_2 are the Fourier coefficients of the modulated signal measured by the synthesized dipole. They can be retrieved by applying multilinear fitting on channels $\mathbf{s}(\delta_1)$ and $\mathbf{sp}(\delta_2)$ data over a spacecraft rotation⁷. The term F_Z is the average value of the signal measured by the Z antennas over a given rotation⁸.

NOTE:

- There are 8 observables quantities ($F_0, F_1(\delta_1), F_1(\delta_2), F'_1(\delta_1), F'_1(\delta_2), F_2, F'_2, F_Z$) for 7 independent equations. In the case of unpolarized source, there are only 4 unknown parameters (S, ϕ, θ, γ) to be determined.

3.2.2 Source intensity

The demodulated voltage power spectral density $P = G_0 Z_0 S$ is derived using the equation 29 in Manning & Fainberg (1980):

$$P = 2 \frac{F_Z(R^2 - 2)/2 + F_0}{R^2} \quad (3.21)$$

Determination of the gain G_0 is given in the section 4.

3.2.3 Source azimuth angle

The source azimuth angle ϕ can be deduced from equations 3.18 and 3.19:

$$\cos 2\phi = \frac{2 F_2}{P P_2} \quad (3.22)$$

$$\sin 2\phi = \frac{2 F'_2}{P P_2} \quad (3.23)$$

Which gives

$$\tan 2\phi = \frac{F'_2}{F_2} \quad (3.24)$$

NOTE:

- The azimuth angle ϕ can also be computed from equations 3.16 and 3.17.

⁷See section A.1 for the values of the phase shifts δ_1 and δ_2 for \mathbf{s} and \mathbf{sp} channels respectively.

⁸With the present assumptions, $P_Z(t)$ should remain constant over a given rotation (i.e., $P_Z(t) = F_Z$).

3.2.4 Source colatitude angle

The source colatitude angle θ can be deduced from relations 3.10 and 3.12:

$$\frac{P_2}{P_1} = \frac{F_2 \cos \phi}{F_1 \cos 2\phi} \quad (3.25)$$

Which leads to the solution:

$$\tan \theta = \frac{4 P_2}{R P_1} \cos \delta \quad (3.26)$$

Where P_1 and P_2 can be replaced by the following expressions in the case of an unpolarized source:

$$P_1 = \frac{2}{P} \sqrt{F_1^2 + F_1'^2} \quad (3.27)$$

$$P_2 = -\frac{2}{P} \sqrt{F_2^2 + F_2'^2} \quad (3.28)$$

NOTE:

- The term P_2 must be negative according to 3.12.
- In practice the function $\theta = \pi + \theta$ is applied when $\theta < 0$, in order to keep θ inside the range of values $[0, \pi]$.
- The elevation angle θ_e can be derived from θ using the relation $\theta_e = \theta - \pi$.

3.2.5 Modulation rate

The modulation rate τ can be defined as:

$$\tau = \frac{P_{max} - P_{min}}{P_{max} + P_{min}} \quad (3.29)$$

Where P_{max} and P_{min} are respectively the maximum and minimum signal amplitude over a given spacecraft rotation.

There are actually two maxima and minima over a given rotation:

$$P_{min1} = P_{syn}(\omega t - \phi = 0^\circ) = P(P_0 + P_1 + P_2) \quad (3.30)$$

$$P_{min2} = P_{syn}(\omega t - \phi = 180^\circ) = P(P_0 - P_1 + P_2) \quad (3.31)$$

$$P_{max1} = P_{syn}(\omega t - \phi = 90^\circ) = P(P_0 - P_2) \quad (3.32)$$

$$P_{max2} = P_{syn}(\omega t - \phi = 270^\circ) = P(P_0 - P_2) \quad (3.33)$$

Assuming $P_{max} = \frac{1}{2}(P_{max1} + P_{max2})$, then:

$$P_{max} = P(P_0 - P_2) \quad (3.34)$$

Assuming $\tau = \frac{1}{2}(\tau_{min1} + \tau_{min2})$, where

$$\tau_{min1} = \frac{P_{max} - P_{min1}}{P_{max} + P_{min1}} = \frac{-P_1 - 2P_2}{2P_0 + P_1} \quad (3.35)$$

$$\tau_{min2} = \frac{P_{max} - P_{min2}}{P_{max} + P_{min2}} = \frac{P_1 - 2P_2}{2P_0 - P_1} \quad (3.36)$$

Then

$$\tau = \frac{-4P_0P_2 + P_1^2}{4P_0^2 - P_1^2} \quad (3.37)$$

3.2.6 Source angular radius

Using expressions 3.14 and 3.20 gives⁹:

$$a \cos^2 \gamma + b \cos \gamma + c = 0 \quad (3.38)$$

Where $a = 1$, $b = 1$ and $c = (4 - \frac{12Fz}{P})/(1 - 3 \cos^2 \theta)$.

The second-degrees equation 3.38 can have several roots depending of the values of the discriminant $\Delta = 1 - 4c$.

If $\Delta > 0$ there are two real roots:

⁹The equation 3.38 is only valid when $\theta \neq 0$ or $\theta \neq \pi$.

$$\cos \gamma = \frac{-1 - \sqrt{1 - 4c}}{2} \quad (3.39)$$

Or

$$\cos \gamma = \frac{-1 + \sqrt{1 - 4c}}{2} \quad (3.40)$$

If $\Delta = 0$ there is only one real root:

$$\cos \gamma = -\frac{1}{2} \quad (3.41)$$

If $\Delta < 0$ there is no real root.

Knowing that: (i) the arccos function is only applicable in the interval $[-1, 1]$, (ii) the angular size $2 * \gamma$ of the source cannot be negative and does not exceed π radians¹⁰ (i.e. $|\gamma| = [0, \pi/2]$), then only the solution 3.40 remains valid at the end.

3.3 Source parameters derived from SEP mode data (equatorial dipole)

3.3.1 Basic formulas

The voltage power spectral density $P_{EQ}(t)$ measured at time t and at frequency f by the receiver in the SEP mode (equatorial dipole only) can be expressed as (Manning & Fainberg 1980):

$$P_{EQ}(t) = R^2 P [P_{0E} + P_{2E} \cos 2(\omega t - \phi) + P'_{2E} \sin 2(\omega t - \phi)] \quad (3.42)$$

Where coefficients P_{0E} , P_{2E} and P'_{2E} are:

¹⁰The present DF inversion method is not valid for radio sources larger than π radians. In all cases, the signal modulation rate tends to 0 when the angular size of the source tends to 2π (i.e. isotropic case).

$$P_{0E} = \frac{1}{3} - \frac{D}{24}(1 - 3 \cos^2 \theta) - \frac{Q}{24}[2 - D(1 - 3 \cos^2 \theta) - 6 \cos \gamma \cos 2\theta] \quad (3.43)$$

$$P_{2E} = -\frac{1}{8}D[\sin^2 \theta - Q(2 + 2 \cos \gamma \cos 2\theta + D \sin^2 \theta)] \quad (3.44)$$

$$P'_{2E} = \frac{1}{4}U \cos(1 + \cos \gamma) \quad (3.45)$$

In the case of an unpolarized source the previous terms can be simplified as:

$$P_{0E} = \frac{1}{3} - \frac{D}{24}(1 - 3 \cos^2 \theta) \quad (3.46)$$

$$P_{2E} = -\frac{1}{8}D \sin^2 \theta \quad (3.47)$$

$$P'_{2E} = 0 \quad (3.48)$$

$$(3.49)$$

Equation 3.42 then becomes:

$$P_{EQ}(t) = R^2 P [P_{0E} + P_{2E} \cos 2(\omega t - \phi)] \quad (3.50)$$

Or equivalently:

$$P_{EQ}(t) = F_{0E} + F_{2E} \cos 2\omega t + F'_{2E} \sin 2\omega t \quad (3.51)$$

Where

$$F_{0E} = R^2 P P_{0E} \quad (3.52)$$

$$F_{2E} = R^2 P P_{2E} \cos 2\phi \quad (3.53)$$

$$F'_{2E} = R^2 P P_{2E} \sin 2\phi \quad (3.54)$$

F_{0E} , F_{2E} and F'_{2E} are the Fourier coefficients of the signal measured by the equatorial dipole (i.e., X antennas). They can be retrieved by performing multilinear fitting over a given rotation.

3.3.2 Source intensity

The demodulated voltage power spectral density P can be derived from P_{0E} and P_Z terms¹¹:

$$P = F_Z + 2\frac{F_{0E}}{R^2} \quad (3.55)$$

3.3.3 Source azimuth angle

The source azimuth angle ϕ can be derived from equations 3.53 and 3.54 :

$$\tan 2\phi = \frac{F'_{2E}}{F_{2E}} \quad (3.56)$$

3.3.4 Source colatitude angle

The colatitude angle θ of the source can be obtained from the expressions 3.47, 3.54 and 3.55 and noting $D = (\frac{12F_Z}{P} - 4)/(3\sin^2\theta - 2)$:

$$\sin^2\theta = \frac{4F'_{2E}}{6F'_{2E} + \alpha \sin 2\phi} \quad (3.57)$$

Where $\alpha = 2(R^2F_Z - F_{0E})$

3.3.5 Modulation rate

It can be noted that:

$$P_{min1} = P_{EQ}(\omega t - \phi = 0^\circ) = R^2P(P_{0E} + P_{2E}) \quad (3.58)$$

$$P_{min2} = P_{EQ}(\omega t - \phi = 180^\circ) = R^2P(P_{0E} + P_{2E}) \quad (3.59)$$

$$P_{max1} = P_{EQ}(\omega t - \phi = 90^\circ) = R^2P(P_{0E} - P_{2E}) \quad (3.60)$$

$$P_{max2} = P_{EQ}(\omega t - \phi = 270^\circ) = R^2P(P_{0E} - P_{2E}) \quad (3.61)$$

From relations above and applying the same approach than in the section 3.2.5, the modulation rate τ can be defined as:

¹¹The term P_Z is defined in the equation 3.14.

$$\tau = -\frac{P_{2E}}{P_{0E}} \quad (3.62)$$

3.3.6 Source angular radius

The technique described in the section 3.2.6 can be also applied in the SEP mode data to determinate the angular radius γ .

4 Antenna calibration

This section presents the method to calibrate RAD1 intensity signal from voltage power spectral density P measured by the RAD1 receiver in $\mu V^2/Hz$ into absolute flux density S of the radio source in physical units (i.e., $W/m^2/Hz$).

4.1 Basic formulas

The calibration is based on the method described by Zaslavsky et al. (2011), using the radio galaxy brightness model from Novaco & Brown (1978) as a reference signal.

In this model the radio galaxy brightness B_{gal} in $W/m^2/Hz/sr$ can be expressed as:

$$B_{gal} = B_0(f^{-0.76})e^{-\tau} \quad (4.1)$$

Where $B_0 = 1.38e^{-19}$, $\tau = 3.28(f^{-0.64})$ and f is the frequency in MHz.

The flux density of the radio galaxy S_{gal} in $W/m^2/Hz$ - supposed to be isotropic and measured by a short dipole antenna - is then:

$$S_{gal} = \frac{1}{2}\Omega B_{gal} \quad (4.2)$$

Where $\Omega = 8\pi/3$ is the short dipole directivity pattern (Kraus 1966). The averaging factor $1/2$ is needed in the case of an unpolarized source.

The expressions 4.2 above and A3 in Zaslavsky et al. (2011) lead to:

$$P_{gal} = Z_0 l_{eff}^2 \Gamma^2 S_{gal} \quad (4.3)$$

Where l_{eff} is the effective length of the short dipole. $\Gamma^2 = |Z_s/(Z_a + Z_s)|^2$ with Z_a and Z_s are the antenna impedance and the stray impedance determined by the spacecraft design, respectively.

NOTE:

- Since at frequencies well above the kHz, the resistive part of these impedances is negligible, the factor Γ can be reduced to $\Gamma = Ca/(Ca + Cs)$, where C_a and C_s are the antenna and the stray capacitances.
- We can notice that $G_0 = l_{eff}^2 \Gamma^2$.

4.2 Antenna calibration steps

The main steps of the calibration are:

1. Estimate the radio background P_{bg} by computing the 5% percentile of the demodulated signal P at each frequency. This step is performed for each day of data between 1995-01-01 and 2019-12-31.
2. Calibration must be performed on three different periods because the equatorial antennas [X] has been partially broken twice since the beginning of the mission. For the three periods an averaged value of P_{bg} is estimated at each frequency¹.
3. The antenna gain $G = G_0 Z_0$ of the short dipole can be then defined by $G = P_{gal}/S_{gal}$, where $P_{gal} = P_{bg} - P_{rec} - P_{noise}$ with P_{rec} and P_{noise} are respectively the receiver² and shot noise³ backgrounds.
4. The radio source flux density S can be then derived using the relation (Zarka et al. 2004): $S = (P - P_{bg})/G$.

NOTE:

- The value of the gain G must be determined separately in SUM mode (synthesized dipole, [X+Z]) and SEP mode (equatorial dipole, [X]).
- The gain ratio R is a function of the equatorial antenna length L_x , also defined as L_{\perp} in Manning & Fainberg (1980). The value of R needs hence to be updated by a factor F after each X antenna break, in order to take account of the new antenna length. The factor F is proportional to L'_x/L_x , where L_x and L'_x are respectively the antenna length before and after the break.

¹See for instance the red dashed lines in the figure 4 for $\langle P_{bg} \rangle$ value at 1040 kHz.

²The receiver background was measured for each frequency, channel (**s**, **sp** and **z**) and acquisition mode (SUM, SEP) just after the launch and before the antenna deployments. In practice it is already removed from input L2 RAD1 data on which DF inversion algorithm is applied.

³The shot noise amplitude - proportional to $(f_{min}/f)^2$ - becomes not significant w.r.t. to galaxy emission above $\sim 500kHz$

- The galaxy background contribution P_{gal} decreases significantly below $\sim 500\text{kHz}$, hence only frequencies in range $[500 - 1040\text{kHz}]$ are used in practice to determine G value.

Figure 4.1 shows the average RAD1 spectra obtained from **s** channel data acquired in SUM mode. Spectra are computed from daily 5% percentile backgrounds over the 3 periods of time (i.e., before, between and after each X antenna break). The yellow dashed line is a simple model of the shot noise. The red dashed line is the galaxy model flux density S_{gal} corrected from the gain factor $1/G$. The receiver background P_{rec} is already removed from the plotted data.

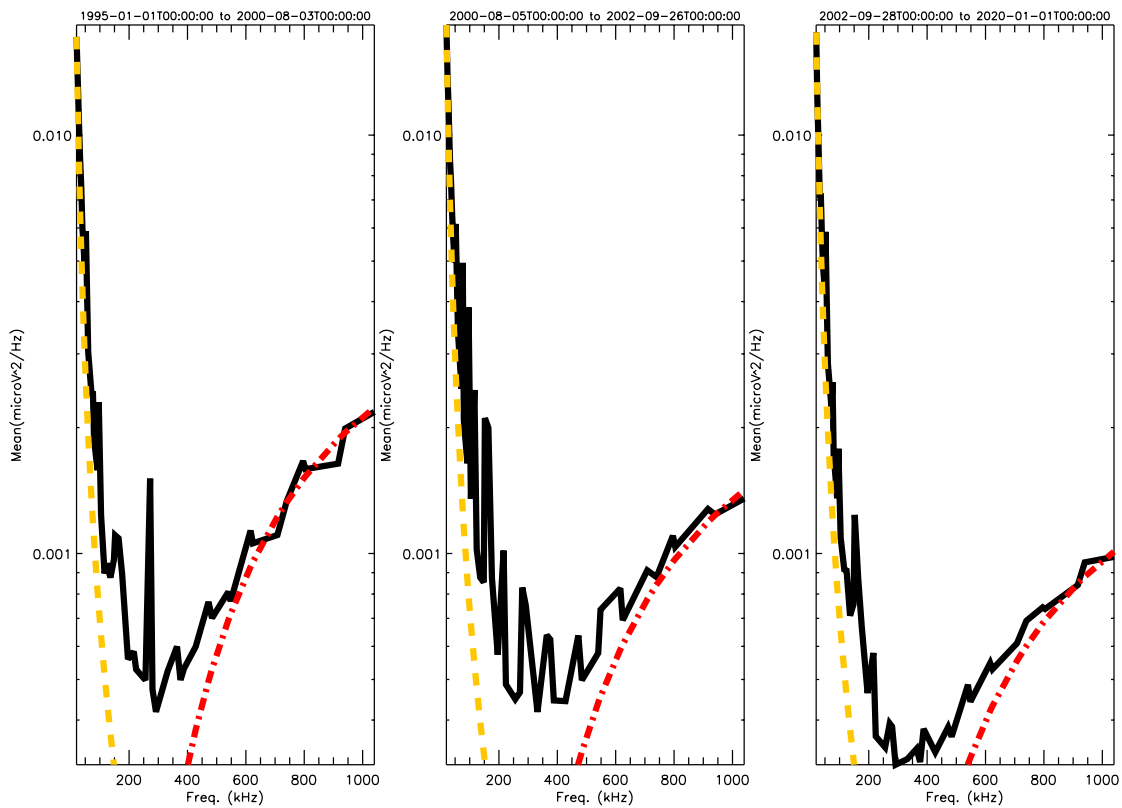


Figure 4.1: Average RAD1 spectra computed from **s** channel data in SUM mode for 3 periods of time (from left to right: before, between and after each X antenna break).

Resulting G values for RAD1 data in SUM mode (synthesized dipole) are given in the table 1.

Appendices

A DF computational data

A.1 Input data overview

The Wind/Waves RAD1 L2 high resolution data produced at LESIA is used as inputs of the DF algorithm. They contains voltage power spectral density in $\mu V^2.Hz^{-1}$, measured by the RAD1 receiver on **s**, **sp** and **z** channels. Following parameters are also needed to perform the inversion such as the **s**, **sp** and **z** sample times (given in seconds since the beginning of the day) or frequencies (in kHz) are also provided. Only L2 data when the RAD1 receiver is in the LIST mode are used. Algorithm is not designed to work with other receiver modes and corresponding data are ignored. A complete description of the L2 data can be found in Bonnin et al. (2021). Table 1 gives the name, definition and values of input static parameters used in the direction-finding algorithm.

A.2 Output data overview

The radio source parameters returned by the method are:

- The absolute flux density S in $W/m^2/Hz$ of the radio source
- The azimuth angle ϕ in degrees of the radio source in a radial-tangent normalized (RTN)-like reference frame (see section B.2 for a definition of this frame)
- The elevation angle θ in degrees of the radio source in a radial-tangent normalized (RTN)-like reference frame
- The source angular radius γ , assuming an extended conical source with uniform brightness
- The modulation rate τ of the signal due to the spacecraft rotation

The inversion returns the intensity value at receiver level, as written in input L2 data (i.e., $\mu V^2/Hz$). The technique used to calibrate the absolute flux density in $W/m^2/Hz$ is detailed in the chapter 4.

Name	Definition	Value(s)
Z_tilt_angles	Tilt angles $[\sigma_a, \sigma_b]$ in degrees of the Z dipole, as defined in Fainberg et al. (1985)	$[0, 0]$
R	Gain ratio between equatorial [X] and radial [Z] antennas. The initial value is known from tests performed on ground before flight (S.Hoang, private communication).	4.5
δ_1	Phase shift in degrees measured for s channel	-178.0
δ_2	Phase shift in degrees measured for sp channel	-90.0
sun_angle_offset	Angular offset in degrees between the X dipole direction and the $X = 0^\circ$ direction in the spacecraft reference frame (see appendix B.1 for more details)	45.0°
G	Antenna gain ($G_0 Z_0$) of the synthesized dipole. Used to convert flux density in $W/m^2/Hz$ from voltage power spectral density in $\mu V^2.Hz^{-1}$. Obtained applying the method described in the section 4 on SUM mode data. There are three values: one before, one between and one after each X antenna break	$[9.754e^{+16} \pm 1.8e^{+14}, 6.194e^{+16} \pm 1.2e^{+14}, 4.4180e^{+16} \pm 3.0e^{+13}]$

Table 1: DF computational inputs.

A complete description of the L3 DF data generated from the inversion method can be found in Bonnin et al. (2021).

B Reference frames

B.1 Wind spacecraft reference frame

The Wind spacecraft reference frame is presented in the figure 2, adapted from Sitruk & Manning (2003).

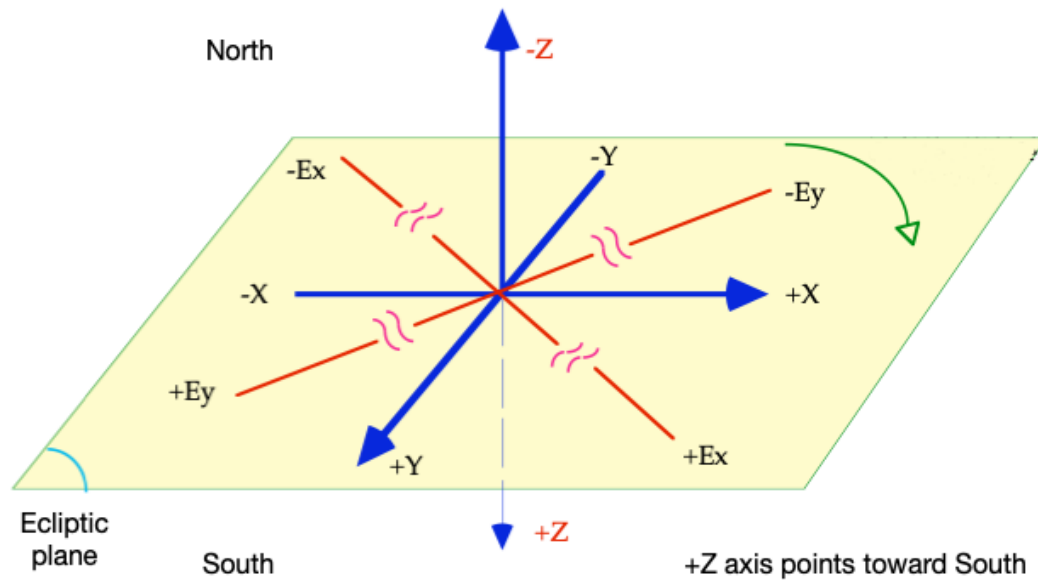


Figure 2: Wind spacecraft reference frame.

It is centered in the spacecraft barycenter, with the X, Y and Z axis defined as follows:

- Z-axis is aligned with the spin axis of the spacecraft, pointing towards the South hemisphere of the Ecliptic plane
- X-axis is in the rotation plane of the spacecraft (also named equatorial plane), pointing towards the magnetometer boom

- Y-axis completes the orthogonal right-handed coordinate system

The direction of rotation of the satellite is direct around the +Z axis oriented to the South.

The electrical antennas $\pm E_x$, $\pm E_y$, and $\pm E_z$ of the Waves experiment are indicated in red⁴. The equatorial antennas $\pm E_x$ and $\pm E_y$ in the rotation plane are not aligned with the X,Y coordinate system of the satellite, but are shifted by a 45° offset angle. The $\pm E_z$ axial antennas are aligned with the spinning axis.

A more detailed description of the Wind spacecraft reference frame and the Waves antennas can be found in Sitruk & Manning (2003).

B.2 Reference frame used for DF output angles

The reference frame used in L3 DF data to define the source azimuth ϕ and elevation θ_e angles is close to a Radial-Tangent Normal frame (RTN), as illustrated in the figure 3.

This "RTN-like" reference frame is centered on the spacecraft barycenter, with the X, Y and Z axis defined as follows:

- Z-axis is aligned with the spin axis of the spacecraft, pointing towards the North hemisphere of the Ecliptic plane
- X-axis is in the Ecliptic plane, pointing towards the Sun center
- Y-axis completes the orthogonal right-handed coordinate system (i.e., Y values are positive in the Sun East side).

In this reference frame the azimuth and elevation angles of the source can be defined as:

$$\phi = \arctan(Y_s, X_s) \tag{4}$$

$$\theta_e = \arctan(Z_s, \sqrt{X_s^2 + Y_s^2}) \tag{5}$$

$$\tag{6}$$

Where X_s , Y_s and Z_s are the cartesian coordinates of the source in the RTN-like frame.

⁴Lengths of the antennas are not representative in the figure.

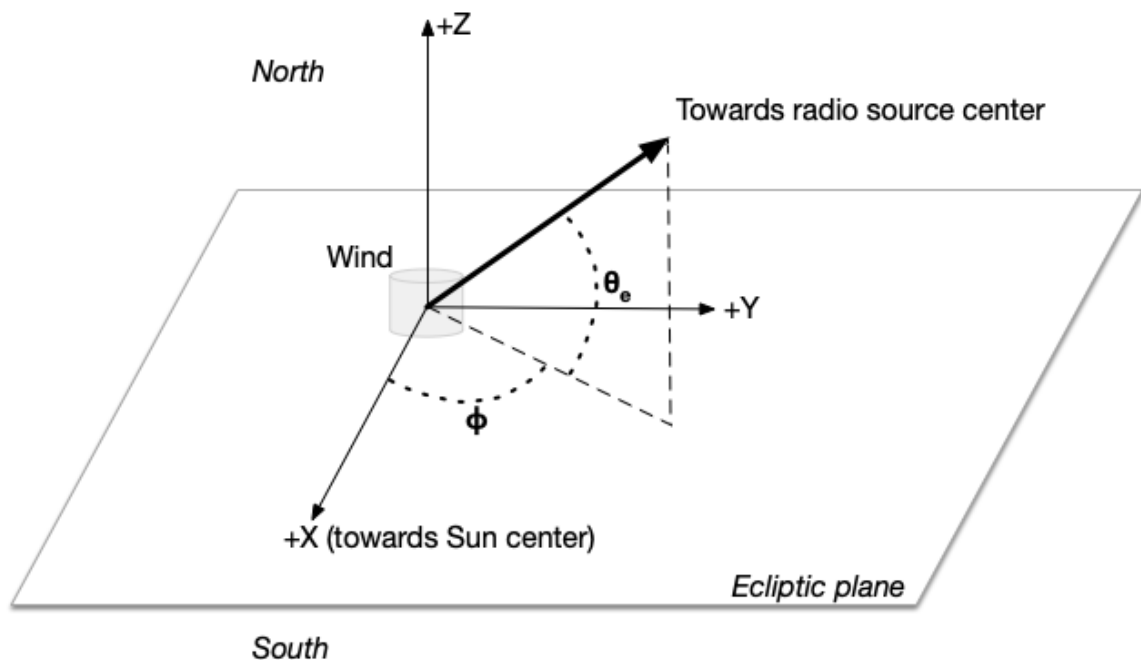


Figure 3: DF output angles reference frame.

C Determination of effective antenna length for synthesized dipole

C.1 Analysis of signal amplitude over time

Figure 4 gives the voltage power spectral density P_{syn} measured by the RAD1 receiver in the SUM mode (synthesized dipole) at 1040 kHz between the 1st of January 1995 and 31st of December 2019. There is one data point per day representing the 5% percentile value computed at this frequency over 24h. The X-axis gives the dates. The Y-axis is the voltage power spectral density $\langle P_{syn} \rangle_{>5\%}$ in $\mu V^2/Hz$. The receiver noise P_{rec} is already removed from data.

It can be noticed:

- Two significant changes in the mean amplitude occurred: a first one around midnight between 3rd and 4th of August 2000 and a second one on 25th of September 2002 just before 2:30 AM. It is admitted that these changes are

C. DETERMINATION OF EFFECTIVE ANTENNA LENGTH FOR SYNTHESIZED DIPOLE25

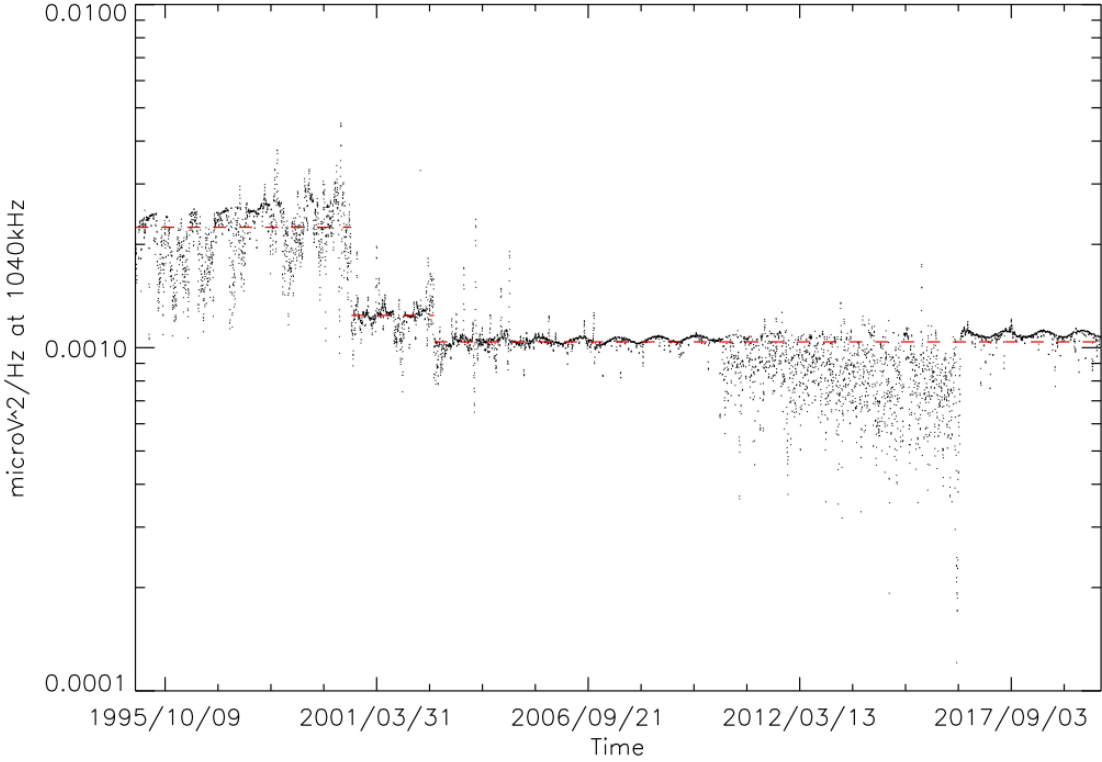


Figure 4: 5% percentile daily amplitude of the RAD1 SUM mode data at 1040 kHz between 1995-01-01 and 2019-12-31. (The receiver noise P_{rec} is already removed from data.)

due to breaks of the X antennas (may be caused by collisions with micro-meteoroids).

- A 1-year amplitude fluctuation of $\sim 12\%$ is visible. This modulation tends to disappear when the frequency decreases. Possible causes of this effect is discussed in Briand, C. and Bougeret, J.-L. (2011).
- A drift of the RAD1 receiver signal is observed with the time. The magnitude of the drift is $0.02 \mu V.Hz^{-1/2}$ per day before the first antenna cut and $3.10^{-7} \mu V.Hz^{-1/2}$ after (Briand, C. and Bougeret, J.-L. 2011).

The 3 red dashed lines are the mean amplitude values respectively computed: (i)

before the first X antenna break, (ii) between the first and second breaks, (iii) after the second break. They correspond to the three P_{bg} values used to calibrate data (see section 4).

C.2 Effective antenna length for synthesized dipole

Table 2 gives estimations of the antenna effective length L_{syn} (in meter) of the synthesized dipole from several studies.

A rough estimation of the antenna length L_{syn} after each break can be also deduced by assuming $L_{syn} = L_X / \cos(\pi/2 - \arctan R) \approx 51.2 m$ before the first cut and noting $P_{syn} \propto L_{syn}^2$. Hence, the antenna length L'_{syn} after a break is close to $L'_{syn} \approx L_{syn} \sqrt{P'_{syn}/P_{syn}}$, where P'_{syn} is the voltage power spectral density measured after the break⁵.

NOTE:

- The synthesized dipole [X+Z] is similar to a physical dipole inclined of an angle of $\arctan(R)$ from the spin-axis. The X antenna length L_X is hence linked to the synthesized dipole length L_{syn} by the relation $L_X/L_{syn} = \cos(\pi/2 - \arctan R)$. For $R \sim 4.5$ (value obtained during ground tests before the launch), the synthesized dipole makes an angle of $\sim 77^\circ$ with the spin-axis and the ratio L_X/L_{syn} is very close to 1.

C.3 Waves antenna facts

Table 3 gives Wind/Waves antennas initial characteristics (i.e., before X antenna breaks and Z antenna extension deployment). As a reminder, $\Gamma = Ca/(Ca + Cs)$, where C_a and C_s are the antenna and the stray capacitances.

⁵In practice the average values $\langle P_{syn} \rangle$ and $\langle P'_{syn} \rangle$ over each period and for a given frequency range (i.e., $f > 800 kHz$) are used.

C. DETERMINATION OF EFFECTIVE ANTENNA LENGTH FOR SYNTHESIZED DIPOLE27

Methods applied	L_{syn} before the first X antenna break	L_{syn} between the two X antenna breaks	L_{syn} after the second X antenna break
From comparison with S/waves data (Krupar, V. and Cecconi, B. and Hoang, S. and Maksimovic, M. and Santolik, O and Zaslavsky, A. 2011)	66	N/A	37
Applying galaxy model method on CDPP RAD1 60-seconds averaged data (Krupar, V. and Cecconi, B. and Hoang, S. and Maksimovic, M. and Santolik, O and Zaslavsky, A. 2011)	66	N/A	41
Applying galaxy model method on RAD1 L2 high resolution data (Bonnin, private communication)	52 ± 1.5	39.7 ± 1.6	36.5 ± 1.5
Using P_{syn} ratio after/before X antenna break (see appendix C.2)	51	40	34

Table 2: Synthesized dipole effective length in meters.

Antenna	C_a (pF)	C_s (pF)	Γ	l_{eff} (m)	Γl_{eff} (m)
X	122	20	0.8592	50	42.9577
Y	22.0	19.0	0.5365	7.5	4.02439
Z	30	45	0.4	4.3	1.72

Table 3: Antenna parameters.

Bibliography

- Bonnin, X., Hoang, S., Cecconi, B., & Issautier, K. 2021, PROPOSITION D'ARCHIVAGE AU CDPP DES DONNEES RADIO WIND/WAVES: Description des jeux de données, Tech. rep., LESIA
- Bougeret, J.-L., Kaiser, M. L., Kellogg, P. J., et al. 1995, *Space Science Reviews*, 71, 231
- Briand, C. and Bougeret, J.-L. 2011, Apparent annual fluctuation of the galactic background on WIND et STEREO, personal communication
- Dulk, G. A., Erickson, W. C., Manning, R., & Bougeret, J. L. 2001, *A&A*, 365, 294
- Fainberg, J., Hoang, S., & Manning, R. 1985, *A&A*, 153, 145
- Kraus, J. D. 1966, *Radio astronomy*
- Krupar, V. and Cecconi, B. and Hoang, S. and Maksimovic, M. and Santolik, O and Zaslavsky, A. 2011, Inter Calibration between STEREO/Waves and Wind /Waves, personal communication
- Manning, R. & Fainberg, J. 1980, *Space Science Instrumentation*, 5, 161
- Novaco, J. C. & Brown, L. W. 1978, *ApJ*, 221, 114
- Sitruk, L. & Manning, R. 2003, L'expérience spatiale G.G.S. / WIND / WAVES Ondes radioélectriques et ondes de plasma, Tech. rep., DESPA
- Waters, J. E., Jackman, C. M., Lamy, L., et al. 2021, *Journal of Geophysical Research (Space Physics)*, 126, e29425
- Zarka, P., Cecconi, B., & Kurth, W. S. 2004, *Journal of Geophysical Research (Space Physics)*, 109, A09S15
- Zaslavsky, A., Meyer-Vernet, N., Hoang, S., Maksimovic, M., & Bale, S. D. 2011, *Radio Science*, 46, RS2008